

## A MASSIVE NEUTRON STAR IN THE GLOBULAR CLUSTER M5

PAULO C. C. FREIRE<sup>1</sup>, ALEX WOLSZCZAN<sup>2</sup>, MAUREEN VAN DEN BERG<sup>3</sup>, JASON W. T. HESSELS<sup>4</sup>

*Draft version November 6, 2018*

### ABSTRACT

We report the results of 19 years of Arecibo timing for two pulsars in the globular cluster NGC 5904 (M5), PSR B1516+02A (M5A) and PSR B1516+02B (M5B). This has resulted in the measurement of the proper motions of these pulsars and, by extension, that of the cluster itself. M5B is a 7.95-ms pulsar in a binary system with a  $> 0.13 M_{\odot}$  companion and an orbital period of 6.86 days. In deep HST images, no optical counterpart is detected within  $\sim 2.5\sigma$  of the position of the pulsar, implying that the companion is either a white dwarf or a low-mass main-sequence star. The eccentricity of the orbit ( $e = 0.14$ ) has allowed a measurement of the rate of advance of periastron:  $\dot{\omega} = (0.0142 \pm 0.0007)^{\circ}\text{yr}^{-1}$ . We argue that it is very likely that this periastron advance is due to the effects of general relativity, the total mass of the binary system then being  $(2.29 \pm 0.17) M_{\odot}$ . The small measured mass function implies, in a statistical sense, that a very large fraction of this total mass is contained in the pulsar:  $M_p = (2.08 \pm 0.19) M_{\odot}$  ( $1 \sigma$ ); there is a 5% probability that the mass of this object is  $< 1.72 M_{\odot}$  and a 0.77% probability that  $1.2 M_{\odot} \leq M_p \leq 1.44 M_{\odot}$ . Confirmation of the median mass for this neutron star would exclude most “soft” equations of state for dense neutron matter. Millisecond pulsars (MSPs) appear to have a much wider mass distribution than is found in double neutron star systems; about half of these objects are significantly more massive than  $1.44 M_{\odot}$ . A possible cause is the much longer episode of mass accretion necessary to recycle a MSP, which in some cases corresponds to a much larger mass transfer.

*Subject headings:* binaries: general — pulsars: general — pulsars: individual (PSR B1516+02A) — pulsars: individual (PSR B1516+02B) — neutron stars: general — equation of state: general

### 1. INTRODUCTION

Over the past 21 years, more than 130 pulsars have been discovered in globular clusters (GCs)<sup>5</sup>. Among the first discoveries were PSR B1516+02A and PSR B1516+02B (Wolszczan et al. 1989). Both are located in the GC NGC 5904. This cluster is also known as M5 and we refer to these pulsars below as M5A and M5B. M5A is an isolated millisecond pulsar (MSP) with a spin period of 5.55 ms. M5B is a 7.95-ms pulsar in a binary system with a low-mass companion (see §5.2) and an orbital period of 6.86 days. At the time of its discovery, this was the MSP with the most eccentric orbit known ( $e = 0.14$ ), this being  $\sim 10^4 - 10^5$  times larger than that of MSP-White Dwarf (WD) systems in the Galactic disk with similar orbital periods.

In the Galactic disk, 80% of all known MSPs are found to be in binary systems and, with the single exception of PSR J1903+0327 (Champion et al. 2008), they are in low-eccentricity orbits with WD companions. In GCs, gravitational interactions with neighboring stars, or even exchange encounters, can produce binary systems with

eccentric orbits (Rasio & Heggie 1995). These high eccentricities allow the measurement of post-Keplerian parameters such as the rate of advance of periastron ( $\dot{\omega}$ ) or, in the future, the Einstein delay ( $\gamma$ ) that are not normally measurable in MSP binaries in the Galactic disk. If these effects are relativistic, they allow estimates of the the total binary and component masses.

When Anderson et al. (1997) published timing solutions for M5A and B they used the eccentricity of M5B to detect its periastron advance. However, the large relative uncertainty of the measurement did not allow any astrophysically useful constraints on the total mass of the binary. In this paper we report the results of recent (2001 to 2008) 1.1-1.6 GHz (L-band) observations of M5. The first 2001 observations were part of an Arecibo search for pulsars in GCs, which found 11 new MSPs (Hessels et al. 2007). Three of these were found in M5, and subsequent observations of this GC were made chiefly with the aim of timing these new discoveries (Stairs et al. 2008, in preparation). M5A and B are in the same radio beam as the new pulsars and they are clearly detectable in the L-band data, permitting timing (see Figs. 1 and 2) of much better (M5A) or comparable (M5B) quality to that obtained at 430 MHz by Anderson et al (1997). The whole dataset now spans nearly 19 years and provides much improved timing parameters.

### 2. OBSERVATIONS, DATA REDUCTION AND TIMING

M5A and B were observed with the Arecibo 305-m radio telescope from the time of their discovery in 1989 April until 1994 July using the 430-MHz Carriage House line feed. For this, a 10-MHz band centered at 430 MHz was used. The Arecibo correlation spectrometer made a

<sup>1</sup> N.A.I.C., Arecibo Observatory, HC 03 Box 53995, PR 00612, U.S.A.; pfreire@naic.edu

<sup>2</sup> Department of Astronomy and Astrophysics, Penn State University, University Park, PA 16802, U.S.A.; alex@astro.psu.edu

<sup>3</sup> Harvard-Smithsonian Center for Astrophysics, 60 Garden Street, Cambridge, MA 02138, U.S.A.; maureen@head.cfa.harvard.edu

<sup>4</sup> Astronomical Institute “Anton Pannekoek”, University of Amsterdam, Kruislaan 403, 1098 SJ Amsterdam, The Netherlands; jhessels@science.uva.nl

<sup>5</sup> For an updated list, see [http://www2.naic.edu/\\$\sim\\$pfreire/GCpsr.html](http://www2.naic.edu/$\sim$pfreire/GCpsr.html).

3-level quantization of the signal and correlated this for a total of 128 lags. These data were then integrated for  $506.58561 \mu\text{s}$ , and the orthogonal polarizations added in quadrature before being written to magnetic tape. The L-band observations began in 2001 June, using the “old” Gregorian L-Wide receiver ( $T_{sys} = 40 \text{ K}$  at 1400 MHz). The “new” L-Wide receiver ( $T_{sys} = 25 \text{ K}$  at 1400 MHz) has been used since it was installed in the Gregorian dome in 2003 February. The Wide-band Arecibo Pulsar Processors (WAPPs, Dowd, Sisk & Hagen 2000) make a 3-level digitization of the voltages over a 100-MHz band for both (linear) polarizations, autocorrelating these for a total of 256 lags. The data are then integrated for a total of  $64 \mu\text{s}$  and the orthogonal polarizations added in quadrature and written to disk. At first, only one WAPP was available, and centered the observing band at 1170 MHz or 1425 MHz. From 2003, three more WAPPs have been available, and we now use three of them to observe simultaneously at 1170, 1410 and 1510 MHz, the cleanest bands within the wide frequency coverage of the new L-Wide receiver.

For all observations, the lags were Fourier transformed to generate power spectra. For the L-band observations, the power spectra were partially dedispersed at a dispersion measure (DM) of  $29.5 \text{ cm}^{-3}\text{pc}$  and stored as a set of 16 sub-bands on the disks of the Borg computer cluster at McGill University. At 1170 MHz, the partial dedispersion introduces an extra smearing of 18 and  $1.6 \mu\text{s}$  for M5A and B respectively. Adding these values in quadrature to the dispersive smearing per channel (60.9 and  $59.7 \mu\text{s}$  respectively), we obtain a total dispersive smearing of 63.5 and  $59.7 \mu\text{s}$  for M5A and B respectively, i.e., the sub-banding introduces very little extra smearing. The 430-MHz power spectra and L-band sub-bands were dedispersed at the known DM of these pulsars and folded modulo their spin periods. All the L-band data reported in this paper were processed using the PRESTO pulsar software package<sup>6</sup>.

We added the best 1170 MHz detections of both pulsars to derive “standard” pulse profiles, and these are displayed in Figure 1. A minimal set of Gaussian curves were fitted to these profiles to derive synthetic templates for each pulsar, and these were then cross-correlated with each observation’s pulse profile in the Fourier domain (Taylor 1992) to obtain topocentric times of arrival (TOAs). Adding all the 1170 MHz observations irrespective of their signal-to-noise ratio (SNR, this varies from day to day because of diffractive interstellar scintillation), we obtain a “global” pulse profile which has a lower SNR than the “standard” pulse profile. We calculated the average flux densities for both pulsars (see Table 1) from the off-pulse r.m.s. in their global profile, assuming a system equivalent flux density of  $3.5 \text{ Jy}$  which is valid for 1170 MHz at the high zenith angles required to observe M5.

The TOAs were analyzed with TEMPO<sup>7</sup>, using the DE 405 Solar System ephemeris (Standish 1998) to model the motion of the Arecibo radio telescope relative to the Solar System Barycenter. The orbital parameters for M5B were modeled using the Damour & Deruelle orbital model (Damour & Deruelle 1985;

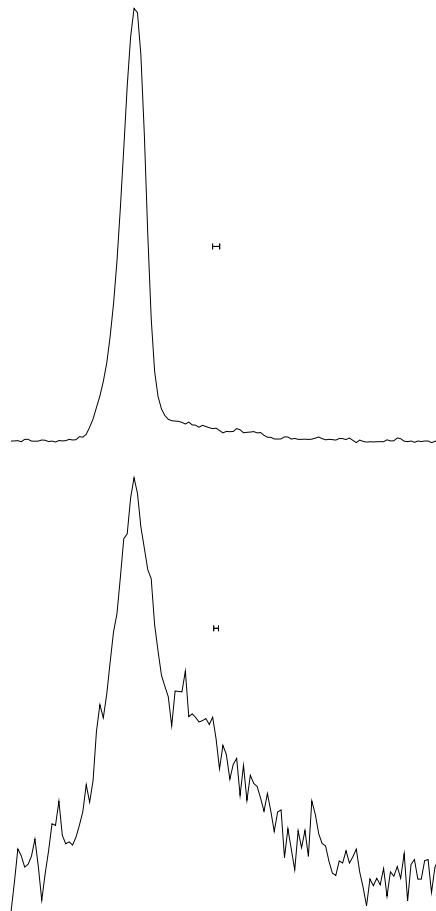


FIG. 1.— Full-cycle pulse profiles for M5A (top) and M5B (bottom) at 1170 MHz, obtained by averaging the best detections of these pulsars at this frequency. The horizontal error bars denote the total time resolution of the system at 1170 MHz: 90.2 and  $87.5 \mu\text{s}$  for M5A and B respectively.

Damour & Deruelle 1986). For most of the early 430-MHz TOAs we have no reliable uncertainty estimates. Therefore, in order to achieve a reduced  $\chi^2$  of 1 for both pulsars, we attributed a constant uncertainty to the 430-MHz TOAs that is similar to their unweighted rms. These times are listed in Table 1. With these TOAs, we obtain timing parameters that are virtually identical to those obtained by the previous analysis (Anderson et al. 1997). For the new L-band data, we find the TOA uncertainties to be under-estimated in the case of M5A. Multiplying these by a factor of about 1.5, we achieve a reduced  $\chi^2$  of 1 for its L-band TOAs. In the case of M5B, this factor is 1.05. These values are similar to those derived for other MSPs timed with the same software (Freire et al. 2008).

The resulting timing parameters and their  $1-\sigma$  uncertainties are presented in Table 1. We estimate these uncertainties to be twice the  $1-\sigma$  Monte-Carlo bootstrap (Efron & Tibshirani 1993; Press et al. 1992) uncertainties. We discuss the validity of this choice for the particular case of the periastron advance of M5B in §5. All the parameters that vary in time ( $\alpha$ ,  $\delta$ ,  $\nu$  and  $\omega$ ) are estimated for the arbitrary epoch, MJD = 54000 (2006 September 22);  $T_0$  was the first periastron passage to occur after that date. The post-fit timing residuals are

<sup>6</sup> <http://www.cv.nrao.edu/~sransom/presto>

<sup>7</sup> <http://www.atnf.csiro.au/research/pulsar/tempo/>

TABLE 1  
PARAMETERS FOR TWO PULSARS IN NGC 5904

Observation and flux parameters	PSR B1516+02A	PSR B1516+02B
Start of 430-MHz observations		47635
End of 430-MHz observations		49432
Number of TOAs @ 430 MHz	86	82
Residual rms @ 430 MHz ( $\mu\text{s}$ )	49	114
Start of L-band observations		52087
End of L-band observations		54497
Number of TOAs @ L-band	1278	162
Uncertainty scale factor <sup>a</sup>	1.50	1.05
Residual rms @ L-band ( $\mu\text{s}$ )	9	72
Average flux density @ 1170 MHz (mJy)	0.155	0.027
Ephemeris		
Reference Epoch (MJD)	54000	54000
Right Ascension, $\alpha$ (J2000)	15 <sup>h</sup> 18 <sup>m</sup> 33 <sup>s</sup> .32307(6) <sup>b</sup>	15 <sup>h</sup> 18 <sup>m</sup> 31 <sup>s</sup> .4625(8)
Declination, $\delta$ (J2000)	+02°05'27".435(3)	+02°05'15".30(3)
Proper motion in $\alpha$ , $\mu_\alpha$ (mas yr <sup>-1</sup> , J2000)	4.6(4)	3.4(1.2)
Proper motion in $\delta$ , $\mu_\delta$ (mas yr <sup>-1</sup> , J2000)	-8.9(1.0)	-11.8(2.8)
Spin frequency, $\nu$ (Hz)	180.063624055103(3)	125.83458757935(6)
Time derivative of $\nu$ , $\dot{\nu}$ (10 <sup>-15</sup> Hz s <sup>-1</sup> )	-1.33874(4)	0.05233(15)
Dispersion Measure, DM (pc cm <sup>-3</sup> )	30.0545(10)	29.46(3)
Orbital period, $P_b$ (days)	...	6.8584538(3)
Projected size or orbit, $x$ (l-s)	...	3.04857(2)
Orbital eccentricity, $e$	...	0.137845(10)
Time of passage through periastron, $T_0$ (MJD)	...	54004.02042(15)
Longitude of periastron, $\omega$ (°)	...	359.898(8)
Rate of advance of periastron, $\dot{\omega}$ (° yr <sup>-1</sup> )	...	0.0142(7)
Second time derivative of $\nu$ , $\ddot{\nu}$ (10 <sup>-27</sup> Hz s <sup>-2</sup> )	[-0.6 ± 0.5] <sup>c</sup>	[4.4 ± 5.4]
Time derivative of $x$ , $\dot{x}$ (10 <sup>-12</sup> l-s/s)	...	[-0.12 ± 0.09]
Time derivative of $P_B$ , $\dot{P}_B$ (10 <sup>-12</sup> )	...	[15 ± 31]
Derived parameters		
Spin period, $P$ (ms)	5.55359254401089(11)	7.946940656275(4)
Time derivative of $P$ , $\dot{P}$ (10 <sup>-21</sup> s s <sup>-1</sup> )	41.2899(13)	-3.306(10)
Mass function, $f$ ( $M_\odot$ )	...	0.000646723(13)
Total system mass, $M$ ( $M_\odot$ )	...	2.29(17)
Maximum pulsar mass, $M_{p,\text{max}}$ ( $M_\odot$ )	...	2.52
Minimum companion mass, $M_{c,\text{min}}$ ( $M_\odot$ )	...	0.13

<sup>a</sup> This is the scale factor for TOA uncertainties required to achieve a reduced  $\chi^2$  of unity in the solution.  
<sup>b</sup> 1- $\sigma$  uncertainties are presented in parenthesis. These are twice the estimate obtained using the Monte-Carlo bootstrap method.  
<sup>c</sup> Values in square brackets are not considered to be significant. They were not fit when determining the remaining timing parameters.

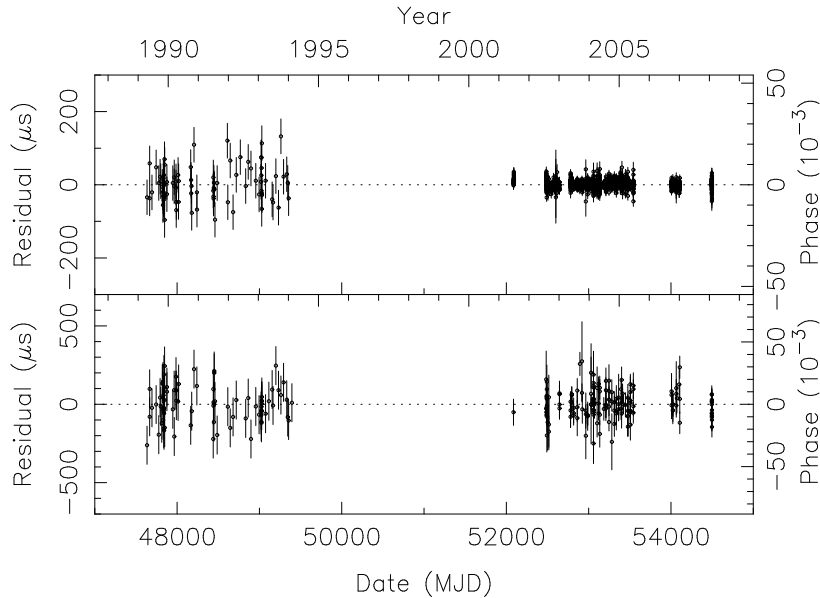


FIG. 2.— Timing residuals for M5A (upper) and M5B (lower), obtained with the ephemerides in Table 1. The large gap in time coverage is mostly due to the Arecibo upgrade.

essentially featureless at the present timing accuracy (see Fig. 2). The large gap without measurements between the early 430-MHz data and later L-band data is in part due to the Arecibo upgrade of the late 1990’s. We included an arbitrary time step between these two datasets in the fit. We have tested the timing solution by introducing extra pulsar rotations between the two datasets, but these are always absorbed by this arbitrary time step, with no other changes in the fitted timing parameters.

The positions, periods and period derivatives that we have obtained are consistent with those of Anderson et al (1997). In what follows, we analyze solely the newly measured parameters: the proper motions and the rate of advance of periastron of M5B.

### 3. PROPER MOTIONS

In the reference frame of a GC, the rms of the velocities of its pulsars along the orthogonal axes perpendicular to the line of sight should be the same as the rms of their velocities along the line of sight. The stellar rms velocity along the line of sight at the center of M5 is  $7.15 \text{ km s}^{-1}$  (Webbink 1985); the rms of the pulsar velocities should be smaller given the larger masses of the neutron stars (NSs). At the distance of M5, 7.5 kpc (Harris 1996), the stellar rms velocity represents a proper motion rms of only  $0.2 \text{ mas yr}^{-1}$ . Given the present measurement precision, the estimated pulsar proper motions should be mutually consistent and reflect only the proper motion of the GC. The proper motion measurements in Table 1 are indeed  $\sim 1\sigma$  consistent with each other; from their weighted average we derive a proper motion for M5 of  $\mu_\alpha = (4.3 \pm 0.4) \text{ mas yr}^{-1}$  and  $\mu_\delta = (-9.6 \pm 1.0) \text{ mas yr}^{-1}$ .

M5 is one of the four GCs in the Galaxy for which optical proper motion measurements have not provided consistent (i.e., agreeing within the formal uncertainty estimates) results (Dinescu, Girard & van Altena 1999). Our M5 proper motion measurement is in marginal agreement with the values derived by Scholz et al. [1996,  $\mu_\alpha = (6.7 \pm 0.5) \text{ mas yr}^{-1}$  and  $\mu_\delta = (-7.8 \pm 0.4) \text{ mas yr}^{-1}$ ], but is in good agreement with the values derived from Hipparcos [Odenkirchen et al. 1997,  $\mu_\alpha = (3.3 \pm 1.0) \text{ mas yr}^{-1}$  and  $\mu_\delta = (-10.1 \pm 1.0) \text{ mas yr}^{-1}$ ].

### 4. SEARCH FOR THE OPTICAL COUNTERPART OF M5B

We have used the astrometric information on M5B to search for an optical counterpart in archival *HST* ACS/WFC data from programs GO 10120 and GO 10615. The GO-10120 images were taken on 2004 August 1 through the F435W, F625W and F658N filters. Since the uncertainty in the absolute astrometry of *HST* data is  $1\text{--}2''$ , we first tie the astrometry of the GO-10120 ACS images to the ICRS frame using UCAC2 stars (positional accuracy  $\lesssim 0.070''$  down to the magnitude limit of the UCAC2 catalog, Zacharias et al. 2004). Since UCAC2 standards in the small ACS field ( $3.4' \times 3.4'$ ) are scarce, we use ground-based imaging of M5 to derive secondary standards. We retrieved from the public archive of the 2.5 m Isaac Newton Telescope (INT) a 30-s Sloan-r Wide Field Camera image taken on 2004 June 8 and processed only the chip that contained the core of M5 (field of view  $\sim 23' \times 11'$ ). Astrometric calibration of this image was achieved using 308 UCAC2 stars with positions corrected for proper motion to the epoch of the INT image.

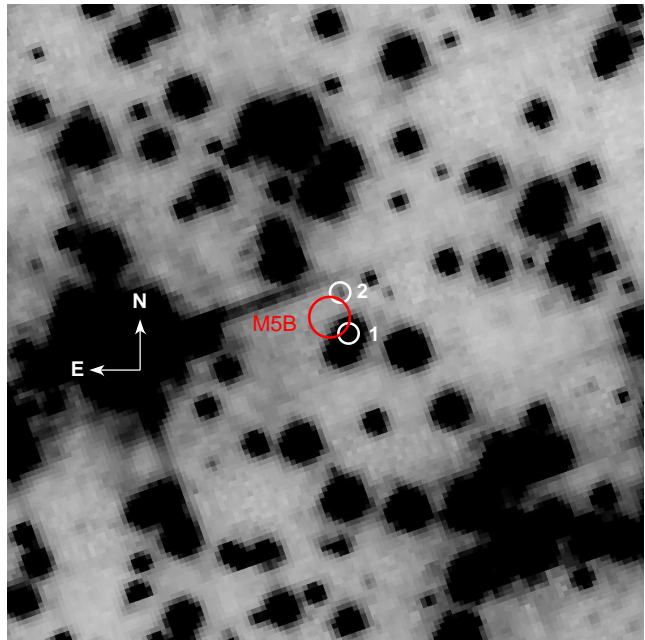


FIG. 3.— A small portion of a GO-10120 *HST* image of M5, centered on the position of M5B, in negative. The picture was taken through the F435W filter of the Advanced Camera for Surveys/Wide Field Camera. The dark circle indicates the position of M5B and the radius ( $0.2''$ ) corresponds to the  $2\sigma$  uncertainty in the absolute astrometry of the image. The nearest stars (white circles) lie at  $2.7$  and  $3.0\sigma$  from the radio position; these are indicated as A and B and are discussed in §4.

After fitting for shift, rotation angle, scale factor and distortions, the final solution has rms residuals of  $0.050''$  in right ascension and  $0.047''$  in declination. We selected a set of 198 secondary standards from unsaturated and relatively isolated stars in the INT image. These were used in turn to compute an astrometric solution for the short (70s) F435W distortion-corrected (using the *multidrizzle* software) exposure. The resulting fit for shift, rotation angle and scale factor has rms residuals of  $0.017''$  in right ascension and  $0.014''$  in declination. We estimate the final  $1\sigma$  accuracy of our ACS absolute astrometry as the quadratic sum of the errors in the UCAC2 astrometry, the UCAC2–INT tie and the INT–*HST* tie, i.e.  $0.1''$  (or 2 ACS pixels).

The position of M5B at the epoch of the GO-10120 observations is shown in Fig. 3. No optical sources are detected within the  $2\text{-}\sigma$  error circle of the radio position (this only includes the uncertainty in the absolute astrometry as the uncertainties in the radio position are negligible). The photometry shows the nearest sources—indicated as “1” and “2” at distances  $2.7$  and  $3.0\sigma$ , respectively—to be main-sequence (MS) stars located  $\sim 1.3$  and  $\sim 6.1$  mag (in F435W) below the MS turnoff. Using the M5 turnoff magnitude from Sandquist et al. (1996) and assuming  $B \approx F435W$ , the 14-Gyr isochrones from Bergbusch & Vandenberg (1992) imply that “1” and “2” are  $\sim 0.75$  and  $\sim 0.4M_\odot$  stars, respectively (for a distance modulus  $(m - M) = 14.41$  and  $E(B - V) = 0.03$ , see Sandquist et al 1996). To check for fainter stars, we stacked F435W images taken with fraction-pixel offsets from *HST* program GO 10615 (2006 Feb 15) into a deep (8500 s) high-resolution (twice-oversampled) masterframe. Psf photometry revealed no additional stars within  $3\sigma$  of M5B. A conservative upper

limit for the detection limit is  $m_{F435W} \approx 26 - 26.5$  mag which corresponds to  $\sim 0.25-0.3M_{\odot}$  for MS stars in M5 (although close to star “1” the sensitivity is lower).

In summary, we cannot exclude stars “1” or “2” as counterparts of M5B. However, the astrometry suggests that it is more likely that the true optical counterpart is fainter than our detection limit. That implies that the companion is either a WD or a faint, low-mass MS star.

## 5. PERIASTRON ADVANCE OF M5B

We have determined a highly significant estimate for the rate of advance of periastron of M5B:  $\dot{\omega} = 0.0142(7)^{\circ}\text{yr}^{-1}$ . The  $1\text{-}\sigma$  estimate provided directly by TEMPO is  $\dot{\omega} = 0.01422(43)^{\circ}\text{yr}^{-1}$ . To verify that these values are realistic, we have kept  $\dot{\omega}$  fixed, and fitted all the remaining timing parameters, recording the resulting  $\chi^2$ . Doing this for a range of values of  $\dot{\omega}$ , we obtain the  $1\text{-}\sigma$  uncertainty as the half-width of the region where  $[\chi^2(\dot{\omega}) - \chi^2(\dot{\omega}_{\min}) < 1]$ ,  $\dot{\omega}_{\min}$  being the value that minimizes  $\chi^2$  (Splaver et al. 2002). The result is  $\dot{\omega} = 0.001422(43)^{\circ}\text{yr}^{-1}$ . Estimating all parameters using a Monte-Carlo Bootstrap algorithm (§2) we obtain  $\dot{\omega} = 0.01422(36)^{\circ}\text{yr}^{-1}$ . Furthermore, the lack of significant higher derivatives of the spin frequency (see Table 1) suggests that, with the present timing precision, we are unable to detect any of this pulsar’s timing noise which can contaminate the physical interpretation of its timing uncertainties. This is a necessary pre-condition for an accurate estimation of parameter uncertainties. We therefore believe that the  $1\sigma$  TEMPO uncertainty estimates are essentially accurate. We choose, however, to be more conservative by making our  $1\text{-}\sigma$  uncertainties twice as large as the values suggested by the Monte-Carlo method (see Table 1). This caution is due to our use of two different datasets with a large time gap between them.

This time gap is common to many Arecibo timing data sets, such as that of PSR J0751+1807. Nice et al. (2005) claimed a mass of  $2.1M_{\odot}$  for that pulsar. This claim has recently been retracted, the latest estimate for the pulsar mass now being  $1.26^{+0.14}_{-0.12}M_{\odot}$  ( $1\sigma$ , Nice 2007<sup>8</sup>). The problem with the earlier estimate was not related to the gap as the new estimate is based on essentially the same data. Its cause was the use of a necessarily imperfect ephemeris when folding the very earliest data. This resulted in orbital-dependent smearing of the pulse profiles that led to an error in the calculation of the orbital phase for the earliest data and an over-estimate of the orbital period decay. Because those data were folded online, this problem could only be solved by ignoring the earliest TOAs. Our 430-MHz data contained the signals of more than one pulsar, so we had to record them to tape. This allowed us to re-fold them iteratively after the timing solution had been obtained (Anderson et al. 1997). After updating the timing solution to 2008, we have also re-folded all our L-band data; none of the pulse profiles used in this work are therefore smeared due to imprecise folding.

### 5.1. Is $\dot{\omega}$ relativistic?

The possible contributions to  $\dot{\omega}$  in a system containing a pulsar and an extended star have been studied in

detail by Lai, Bildsten & Kaspi (1995). In their analysis of the binary pulsar PSR J0045–7319 they concluded that the only likely contribution to  $\dot{\omega}$  in such systems is from rotational deformation of the companion. If we assume that PSR J0045–7319 has a mass of  $1.4M_{\odot}$ , the companion mass is  $8.8M_{\odot}$  and its radius  $R_c \sim 6.4R_{\odot}$  (Bell et al. 1995); the orbital separation  $a$  is  $\sim 126R_{\odot}$ . Using these values they reached the conclusion that the contribution to  $\dot{\omega}$  from tidal deformations, which are proportional to  $(R_c/a)^3 \simeq 1.32 \times 10^{-4}$ , is not significant in that system. For M5B, again assuming a pulsar mass of  $1.4M_{\odot}$  with a MS companion of maximum mass  $0.3M_{\odot}$  (see § 4) and a radius  $R_c = 0.3r_{0.3}R_{\odot}$  (where  $r_{0.3} \sim 1$ ), then the orbital inclination  $i$  is  $\sim 24^{\circ}$ ,  $a \sim 18R_{\odot}$  and  $(R_c/a)^3 \simeq 4.5 \times 10^{-6}r_{0.3}^3$ . This is 30 times smaller than for PSR J0045–7319, becoming even less significant for smaller MS companion masses and correspondingly higher inclinations.

Using equations 68 and 79 of Wex (1998) we can estimate the contribution to  $\dot{\omega}$  due to rotational deformation:

$$\dot{\omega}_{\text{rot}} = n \frac{kR_c^2\hat{\Omega}^2}{a^2(1-e^2)^2} \left( 1 - \frac{3}{2} \sin^2 \theta + \cot i \sin \theta \cos \theta \cos \Phi_0 \right), \quad (1)$$

where  $n$  is the orbital angular frequency ( $2\pi/P_b = 1.06 \times 10^{-5}\text{rad s}^{-1}$ ),  $k$  is the gyration radius (for a homogeneous sphere this is 0.63, while for any centrally condensed objects this will always be smaller: it is about 0.2 for a completely convective star),  $\hat{\Omega}$  is the rotation rate relative to break-up,  $\theta$  is the angle between the rotational and orbital angular momenta (if the companion is non-degenerate, these tend to be aligned, so  $\theta = 0$ ) and  $\Phi_0$  is the longitude of the ascending node in a reference frame defined by the total angular momentum vector (see Fig. 9 of Wex 1998).

For the situation discussed above (a  $1.4M_{\odot}$  pulsar with the largest possible MS companion,  $R_c = 0.3r_{0.3}R_{\odot}$ ), we have  $R_c/a = 16.55 \times 10^{-3}r_{0.3}$ . We can also calculate the break-up angular velocity:  $\Omega_{\text{max}} = \sqrt{GM_c/R_c^3} = 1/0.3\sqrt{GM_{\odot}/(r_{0.3}R_{\odot})^3} = 2.09 \times 10^{-3}r_{0.3}^{(3/2)}\text{rad s}^{-1}$ . If the companion’s rotation is tidally locked to its orbit around the pulsar, then  $\hat{\Omega} = n/\Omega_{\text{max}} = 5.06 \times 10^{-3}r_{0.3}^{(3/2)}$ . Therefore,  $\dot{\omega}_{\text{rot}} = 2.65 \times 10^{-15}r_{0.3}^5\text{rad s}^{-1} = 4.79 \times 10^{-6}(r_{0.3}^5)^{\circ}\text{yr}^{-1}$  (or three times this if the companion were to be a homogeneous sphere). This is  $\sim 3 \times 10^3$  times smaller than the value we determined (§5). If the companion were to be significantly distended for its mass (i.e., if  $r_{0.3} > 1$ ), as is the case for the companion of PSR J1740–5340 (Ferraro et al. 2001), then  $\dot{\omega}_{\text{rot}}$  could be significant. This scenario can be excluded, since no optical counterpart is readily detectable within  $\sim 2.5\sigma$  of the pulsar (see §4).

If the companion were to be a WD, then it could be more massive than  $0.3M_{\odot}$  and still evade optical detection. Irrespective of its mass, the contribution to  $\dot{\omega}$  from the tidal deformation of a WD is negligible, but that is not necessarily the case for the contribution from rotational deformation. As an example, we re-calculate  $\dot{\omega}_{\text{rot}}$  for a  $0.3M_{\odot}$  WD. For WDs, we have  $k = 0.45$  (Livio & Pringle 1998), more than twice as large as for fully convective stars. For WDs  $r_{0.3}$  is of the order of 0.1, i.e., the  $(R_c/a)^2$  term in eq. 1 would be  $\sim 10^2$  times

<sup>8</sup> See also <http://www.ns2007.org/talks/nice.pdf>

smaller than discussed for  $r_{0.3} \sim 1$ . However, a WD companion is not likely to be tidally locked. If it were spinning fast, then  $\hat{\Omega} \sim 1$ . While there is no special *a priori* reason why this should be true, it is a possibility that cannot be excluded. This would mean that  $\hat{\Omega}^2$  could be  $\sim 4 \times 10^4$  times larger than discussed above, with  $\dot{\omega}_{\text{rot}}$  similar to the observed  $\dot{\omega}$ . This is particularly so for the larger-sized WDs (those with the lowest masses). Following Splaver et al. (2002), we note first that if the companion is not tidally locked, the angular momenta of the orbit and companion spin will probably not be aligned ( $\theta \neq 0$ ). In this case, the spin of the companion will induce a precession of the orbital plane. This will cause a change in  $i$ , affecting the projected semi-major axis of the orbit which will vary with a rate  $\dot{x}$ . Rewriting equation 81 of Wex (1998), we can relate  $\dot{\omega}_{\text{rot}}$  to  $\dot{x}$ :

$$\dot{\omega}_{\text{rot}} = \frac{\dot{x}}{x} \left( \tan i \frac{1 - \frac{3}{2} \sin^2 \theta}{\sin \theta \cos \theta \sin \Phi_0} + \cot \Phi_0 \right). \quad (2)$$

This equation has the advantage that it does not depend on the mass (or the nature) of the companion. Thus, our observed 2- $\sigma$  upper limit of  $|\dot{x}/x| < 9.6 \times 10^{-14} \text{ s}^{-1}$  implies  $|\dot{\omega}_{\text{rot}}| < (1.7 \times 10^{-4})^\circ \text{ yr}^{-1}$  times a geometric factor. In 80% of cases this geometric factor will be smaller than 10 and the upper limit for  $\dot{\omega}_{\text{rot}}$  is similar to the present measurement uncertainty for  $\dot{\omega}$ .

To summarize,  $\dot{\omega}_{\text{rot}}$  can only be significant if the companion is degenerate, rotating near breakup velocity, and with its rotational angular momentum nearly aligned with the orbital angular momentum, making  $\dot{x}$  undetectable. Otherwise  $\dot{\omega}$  is relativistic.

### 5.2. Binary, pulsar and companion masses

When  $\dot{\omega}$  is solely due to the effects of general relativity, we can measure the total mass of a binary system:

$$M = \left( \frac{P_b}{2\pi} \right)^{5/2} \left[ \frac{(1 - e^2) \dot{\omega}}{3} \right]^{3/2} \left( \frac{1}{T_\odot} \right), \quad (3)$$

where  $T_\odot \equiv GM_\odot/c^3 = 4.925490947 \mu\text{s}$ . For M5B, we obtain  $M = (2.29 \pm 0.17) M_\odot$ . For the nominal value of  $\dot{\omega}$  and a median  $i$  of  $60^\circ$ , the mass of the companion is  $0.173 M_\odot$  and the mass of the pulsar is  $2.11 M_\odot$ . This is well above all NS masses that have been precisely measured to date.

We calculated a 2-D probability distribution function (pdf) for the mass of the pulsar and the mass of the companion, assuming that the pdf for  $\dot{\omega}$  is a Gaussian with the half-width equal to the 1- $\sigma$  uncertainty listed in Table 1 and an *a priori* constant probability for  $\cos i$ . The two-dimensional pdf is then projected in both dimensions, resulting in 1-D pdfs for the mass of the pulsar and the mass of the companion. These are displayed graphically in Fig. 4. The pulsar definitely has a mass smaller than  $2.52 M_\odot$ , and the companion has a mass larger than  $0.13 M_\odot$ , the median and 1- $\sigma$  limits for the pulsar and companion mass are  $2.08^{+0.18}_{-0.19} M_\odot$  and  $0.172^{+0.107}_{-0.023} M_\odot$  respectively. There is a 99%, 95% and 90% probability that the pulsar is more massive than  $1.38$ ,  $1.72$  and  $1.82 M_\odot$  respectively. There is a 0.77% probability that  $i$  is low enough to make the NS mass fall within the range of the components of double neutron star (DNS)

systems: from  $1.20 M_\odot$  measured for the companion of PSR J1756–2251 (Faulkner et al. 2005) to  $1.44 M_\odot$  measured for PSR B1913+16 (Weisberg & Taylor 2003). For M5B, assuming its nominal value of  $\dot{\omega}$ , these mass limits would imply that  $7.9^\circ < i < 10.2^\circ$ .

## 6. STATISTICAL EVALUATION OF MASS MEASUREMENTS

M5B has the second largest mass estimate among all known NSs after PSR J1748–2021B (NGC 6440B). Because of indeterminate orbital inclinations, all mass estimates based solely on  $\dot{\omega}$  are probabilistic statements: one more PK parameter is necessary to have an unambiguous determination of  $i$  and  $M_p$ . No such parameters have yet been measured for M5B, NGC 6440B or any other eccentric MSP binaries in GCs; this is in some cases due to their low timing precision (like M5B, which is faint and has a broad pulse profile), and in others to their small timing baselines (like NGC 6440B). Nevertheless, unambiguous upper limits for the pulsar masses and lower limits for the companion masses can always be obtained from a measurement of a relativistic  $\dot{\omega}$  alone (see Table 2). Furthermore, in systems where the mass function is very small and the total binary mass is very large (as for M5B and NGC 6440B) there is a much greater probability that most of the mass of the binary belongs to the pulsar itself, as described in §5.2.

### 6.1. Evidence for high average neutron star masses

An interesting feature of the eccentric binary MSPs in GCs is that as the binary mass increases, the mass function  $f$  does not increase (see Table 2). The exception is NGC 1851A; a system thought to have resulted from an exchange interaction (Freire et al. 2004). If these binaries were to have  $M_p < 1.44 M_\odot$  then the increase in total mass would be due to higher companion masses, resulting in a general trend to higher mass functions. This is generally not the case.

If we assume that all these GC MSPs have “normal” masses (between 1.2 and  $1.44 M_\odot$ ), we can then calculate the orbital inclinations of these binaries from their total masses and mass functions. These are displayed graphically in Fig. 5. Of the five massive GC systems, four seem to have small orbital inclinations (i.e., with  $\cos i > 0.8$ ), the exception being NGC 1851A. *A priori*, one would expect only one out of five systems to have such a small  $i$ . We have used a Kolmogorov-Smirnov test to compare the  $\cos i$  values corresponding to the nominal  $\dot{\omega}$  values and  $M_p = 1.44 M_\odot$  (only possible to calculate for the five massive binaries) with a fake set of 100 randomly oriented binary systems (i.e., with a uniform distribution of  $\cos i$ ). We obtain a 0.46% probability that the observed distribution is extracted from this set with random orbital orientations. If we use instead  $M_p = 1.2 M_\odot$ , we can calculate  $\cos i$  for all the eccentric GC binaries. The probability that the resulting distribution of  $\cos i$  is selected from the set with random orientations is  $7.7 \times 10^{-5}$ .

Such low inclinations might be less unlikely were there a tendency for pulsars to emit in a plane perpendicular to their orbit. During accretion, orbital angular momentum is transferred to the NS, making its rotation axis nearly perpendicular to its orbital plane. If the angle between the magnetic and rotational axes of pulsars ( $\alpha$ ) is small, the magnetic axis will describe a narrow cone

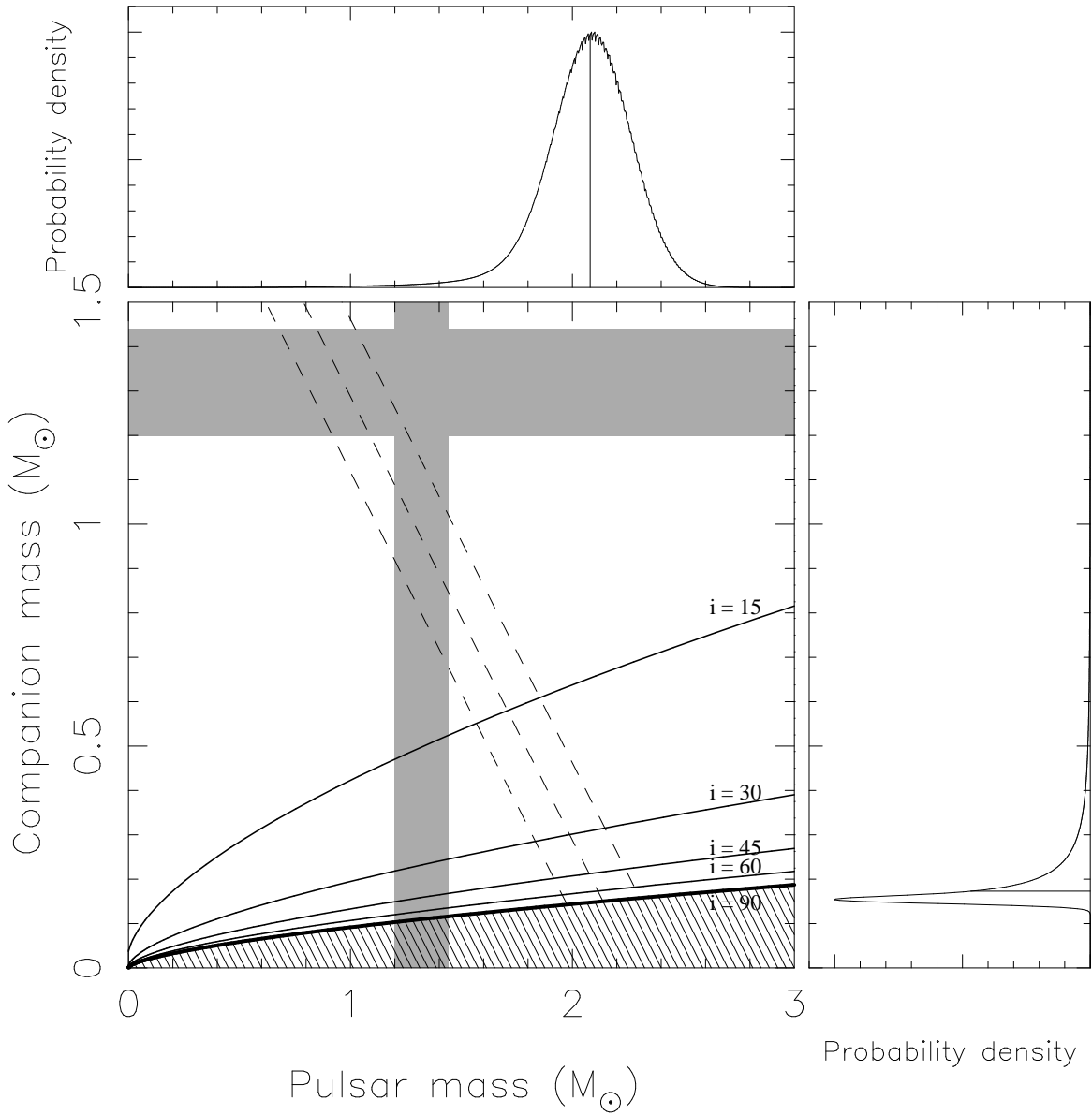


FIG. 4.— Constraints on the masses of M5B and its companion. The hatched region is excluded by knowledge of the mass function and by  $\sin i < 1$ . The diagonal dashed lines correspond to a total system mass that causes a general-relativistic  $\dot{\omega}$  equal to, or within  $1\text{-}\sigma$  of, the measured value. The six solid curves indicate constant inclinations. We also display the probability density function for the mass of the pulsar (*top*) and the mass of the companion (*right*), and mark the respective medians with vertical (horizontal) lines. For comparison, the gray bars indicate the range of “normal” NS masses (see §5.2).

nearly perpendicular to the orbital plane. However, no such tendency for small  $\alpha$  has been described in the literature. If a pulsar has a small  $\alpha$ , its beam will probably illuminate a smaller fraction of the sky, particularly if it is narrow. This can only make the low- $\alpha$  objects *less* likely to be detected<sup>9</sup>. Furthermore, no such tendency towards low orbital inclinations is seen among the two lighter binary MSPs in GCs, nor among the systems with estimated orbital inclinations: NGC 6752A has  $i > 70^\circ$  (Bassa et al. 2006); PSR J1909–3744 has  $i = 86.6(1)^\circ$  (Jacoby et al. 2005; Hotan et al. 2006); PSR J0437–4715 has  $i \sim 43^\circ$  (Verbiest et al. 2008)

<sup>9</sup> The pulse profiles also tend to be wider in these nearly aligned rotators, further hindering their detection. We see no correlation between the “apparent” inclinations in Fig. 5 and the pulse-widths, although the pulsar profile of M5B is quite broad (Fig. 1).

and the massive binary PSR J1903+0327 has  $i \sim 79^\circ$  (Champion et al. 2008)<sup>10</sup>.

If the low mass functions of the massive binaries are not a result of systematically low orbital inclinations, they can only be due to systematically small companion masses. This implies that in the majority of these systems the pulsar masses are significantly larger than in the lighter binaries.

<sup>10</sup> In many cases, high orbital inclinations enable the measurement of the mass of a MSP through Shapiro delay, producing a selection of such inclinations among the systems with measured mass. This should not be too strong in the sample we selected, systems with the timing precision of PSR J1909–3744 and PSR J0437–4715 can have their Shapiro delays measured almost irrespective of their orbital inclination

TABLE 2  
 MILLISECOND PULSAR MASSES

Name PSR	GC	$P$ (ms)	$P_b$ (days)	$e$	$f/M_\odot$	$M/M_\odot^a$	$M_c/M_\odot$	$M_p/M_\odot$	Method <sup>b</sup>	Ref. <sup>c</sup>
Selected MSP Mass Measurements										
J0751+1807	-	3.47877	0.26314	0.00000	0.0009674	-	-	$1.26^{+14}_{-12}$	$P_b, s$	1
J1911-5958A	NGC 6752	3.26619	0.83711	<0.00001	0.002688	$1.58^{+0.16}_{-0.10}$	0.18(2)	$1.40^{+0.16}_{-0.10}$	Opt.	2
J1909-3744	-	2.94711	1.53345	0.00000	0.003122	$1.67^{+3}_{-2}$	0.2038(22)	$1.47^{+3}_{-2}$	$r, s$	3
J0437-4715	-	5.75745	5.74105	0.00002	0.001243	2.01(20)	0.254(14)	1.76(20)	$r, s$	4
J1903+0327	-	2.14991	95.1741	0.43668	0.139607	2.88(9)	1.07(2)	1.81(9)	$\dot{\omega}, s$	5
Binary systems with indeterminate orbital inclinations										
J0024-7204H	47 Tucanae	3.21034	2.35770	0.07056	0.001927	1.61(4)	> 0.164	< 1.52	$\dot{\omega}$	6
J1824-2452C	M28	4.15828	8.07781	0.84704	0.006553	1.616(7)	> 0.260	< 1.367	$\dot{\omega}$	7
J1748-2446I	Terzan 5	9.57019	1.328	0.428	0.003658	2.17(2)	> 0.24	< 1.96	$\dot{\omega}$	8
J1748-2446J <sup>d</sup>	Terzan 5	80.3379	1.102	0.350	0.013066	2.20(4)	> 0.38	< 1.96	$\dot{\omega}$	8
B1516+02B	M5	7.94694	6.85845	0.13784	0.000647	2.29(17)	> 0.13	< 2.52	$\dot{\omega}$	§5.2
J0514-4002A <sup>e</sup>	NGC 1851	4.99058	18.7852	0.88798	0.145495	2.453(14)	> 0.96	< 1.52	$\dot{\omega}$	9
J1748-2021B	NGC 6440	16.76013	20.5500	0.57016	0.000227	2.91(25)	> 0.11	< 3.3	$\dot{\omega}$	10

<sup>a</sup> Binary systems are sorted according to the total estimated mass  $M$ .

<sup>b</sup> Methods are:  $\dot{P}_b$  - relativistic orbital decay,  $r, s$  - Shapiro delay “shape” and “range”, “Opt” - optically derived mass ratio, plus mass estimate based on spectrum of companion,  $\dot{\omega}$  - precession of periastron.

<sup>c</sup> References are 1: (Nice 2007) (total and companion masses not provided), 2: (Bassa et al. 2006), 3: (Hotan et al. 2006), 4: (Verbiest et al. 2008), 5: (Champion et al. 2008), 6: (Freire et al. 2003), 7: (Bégin et al. 2008), 8: (Ransom et al. 2005), 9: (Freire, Ransom & Gupta 2007); 10: (Freire et al. 2008)

<sup>d</sup> This pulsar is not technically a MSP, its spin period is longer than those found in most DNS systems. However, given the similarity of its orbital parameters to those of Terzan 5 I, we assume that it had a similar formation history.

<sup>e</sup> Because of its large companion mass and eccentricity, this system is thought to have formed in an exchange interaction (Freire et al. 2004).

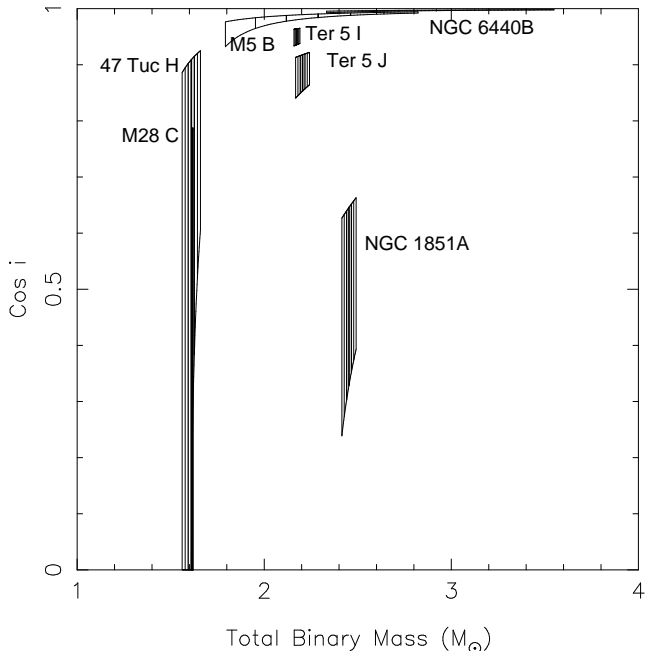


FIG. 5.— Cosine of the orbital inclination  $i$  as a function of total binary mass for the eccentric MSP binaries in GCs. For each binary, the upper curve assumes a pulsar mass of  $1.2 M_\odot$  and the lower curve  $1.44 M_\odot$ . These are different for each binary because of their different mass functions. The vertical lines indicate the total masses corresponding to  $\dot{\omega}$  and its  $\pm 1, 2$  and  $3 - \sigma$  uncertainties, based on the most recent timing. If we assume randomly oriented orbits, then for any given total mass value the vertical distance between the two curves gives us the probability of the pulsar mass falling within the  $1.2 - 1.44 M_\odot$  range. With the exception of NGC 1851A, these probabilities are significantly smaller for the more massive systems.

## 6.2. Implications for the equation of state of dense matter

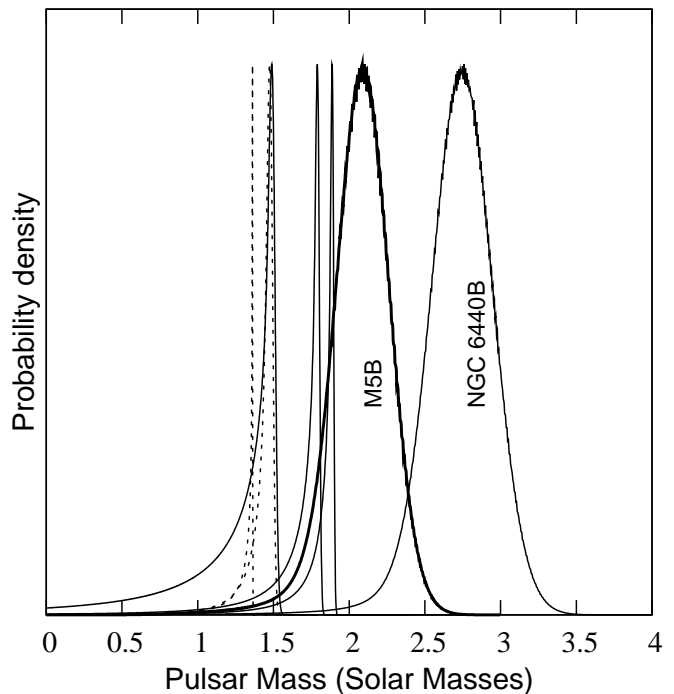


FIG. 6.— Probability distribution functions (pdfs) for the eccentric MSPs binaries in GCs (see also Fig. 5). The mass pdfs of the MSPs in the less massive binaries (those with  $M < 2 M_\odot$ ) are represented by the dashed curves. The distribution of masses is much broader than is found for the components of DNS systems. Four out of a total of seven systems seem to be significantly more massive than the most massive NS in DNS systems, PSR B1913+16.

Because there is no physically plausible reason to assume that most massive binaries have a small  $i$  we now assume that the probability density of  $\cos i$  is constant. We use this to calculate the mass pdfs from  $\dot{\omega}$  as described in § 5.2 for all the pulsars in Fig. 5. The pdfs are



displayed graphically in Fig. 6. If the probability that  $1.2 M_{\odot} < M_p < 1.44 M_{\odot}$  is small (as is the case for Terzan 5 I and J, M5B and NGC 6440B), it is a direct indication that the required orbital inclination ranges are very narrow (as shown in Fig. 5) and therefore unlikely under the present assumption. For M5B, this probability is only 0.77%, while for NGC 6440B it is even smaller, only 0.10%. Multiplying such probabilities for all the massive MSPs in GCs, we obtain a composite probability of  $5.3 \times 10^{-9}$  that all have masses between 1.2 and  $1.44 M_{\odot}$ . It is therefore very likely that some of these NSs are significantly more massive.

As discussed above in §5.2, for M5B there is a 95% probability that the pulsar is more massive than  $1.72 M_{\odot}$ . This would exclude a third of the equations of state considered in Lattimer & Prakash (2007). However, in this respect NGC 6440B should be far more constraining; there are 99 and 95% probabilities that the mass of that pulsar is  $> 2.01$  and  $2.36 M_{\odot}$  respectively. We consider the M5B result to be more secure: the non-detection of its companion (§4) almost guarantees that its  $\dot{\omega}$  is purely relativistic (§5.1).

There are two MSPs listed in Table 2 for which large masses have already been determined, PSR J0437–4715 and PSR J1903+0327. The latter in particular has the potential for a precise, unambiguous measurement of a large pulsar mass in the very near future. At the moment, it has not been confirmed whether its  $\dot{\omega}$  is relativistic or not, although it is likely to be so. These results strengthen the case for the existence of massive NSs.

#### 7. FORMATION OF MASSIVE NEUTRON STARS

The MSP mass estimates in Table 2 and the mass pdfs in Fig. 6, especially those of M5B and NGC 6440B, suggest that the distribution of MSP masses could span a factor of 2, a situation that is completely different to that found for the components of DNSs. NGC 1851A and the MSPs in the “light” ( $M < 2 M_{\odot}$ ) binaries have masses smaller than  $1.5 M_{\odot}$ , i.e., they are not significantly more massive than mildly recycled NSs, despite having spin frequencies of hundreds of Hz. In particular, the case of M28C demonstrated that if all NSs start with  $M_p > 1.2 M_{\odot}$ , then some MSPs can be recycled by accreting  $< 0.15 M_{\odot}$  from their companions. At the other end of the distribution, NGC 6440B could be twice as massive.

It could be that MSPs were born with this wide range of masses. Hydrodynamical core collapse simulations (Timmes et al. 1996; Belczynski et al. 2008) indicate that stars below  $\sim 18 M_{\odot}$  form  $\sim 1.20 - 1.35 M_{\odot}$  NSs (such as 47 Tuc H, M28C and NGC 1851A), while stars with masses between  $18 - 20 M_{\odot}$  form  $1.8 M_{\odot}$  NSs (similar to PSR J0437–4715, PSR J1903+0327, Terzan 5 I, J and M5B). Above  $20 M_{\odot}$ , stars experience partial fall-back of material immediately after the supernova that can significantly increase the mass of the stellar remnant, making it either a super-massive NS (like NGC 6440B) or a black hole.

This possibility raises the question of why such massive NSs, while representing about half of the MSPs in Table 2, have not been found among the 9 known DNS systems. Most of the secondary NSs in DNS systems

have masses between  $1.2$  and  $1.3 M_{\odot}$ , and recently van den Heuvel (2007) suggested that these were formed by electron capture (EC) supernovae. The nine primary NSs in DNS systems were still likely formed in normal (iron core collapse) supernovae. The predicted percentage of massive NSs is quite small, and with only 9 known DNS we are unlikely to see any massive NSs as the primary (Belczynski et al. 2008), a situation that is very different from what is derived for the MSPs.

If the extra mass of some MSPs were instead acquired during the long accretion episodes that recycled them, we can explain naturally why we only see massive NSs as MSPs (not just in GCs, but also in the Galaxy, e.g. Verbiest et al. 2008, Champion et al. 2008) but not in DNS systems.

#### 8. CONCLUSION

We have measured the positions and proper motions of M5A and B. This has allowed a detailed search for the companion of M5B. However, no object was detected within  $2.5\sigma$  of the position of M5B to a magnitude limit of 26–26.5, indicating that its companion is either a low-mass MS star or a WD. We have measured the rate of advance of periastron for this binary system, concluding that it is very likely due solely to the effects of general relativity. In this case, the total mass of the binary is  $2.29 \pm 0.17 M_{\odot}$ , similar to the total masses of Terzan 5 I and J. Like those pulsars and NGC 6440B, the relatively low mass function for M5B indicates that most of the system mass is likely to be in the pulsar, which we estimate to be  $2.08 \pm 0.19 M_{\odot}$  ( $1 \sigma$ ). There is a 95% probability that the mass of this pulsar is above  $1.72 M_{\odot}$ . If confirmed, this would exclude about a third of the equations of state that are now accepted as possible descriptions of the bulk properties of super-dense matter.

Together with other recent results, the large mass derived for M5B suggests that MSPs have a very broad mass distribution; half of these objects seem to be significantly more massive than  $1.44 M_{\odot}$ . It is likely that all NSs began with the a narrow mass range like that found in DNS. They then accreted different amounts of matter (in some cases as much as their starting mass) during their evolution to the MSP phase.

We thank S. M. Ransom and I. H. Stairs for many of the L-band observations made since 2001, Patrick Lazarus and Melissa Iardo for help with data reduction, Chris Salter, Marten van Kerkwijk and the referee, Matthew Bailes, for their many constructive suggestions. J.W.T.H. thanks NSERC and the Canadian Space Agency for a postdoctoral fellowship and supplement respectively. The Arecibo Observatory, a facility of the National Astronomy and Ionosphere Center, is operated by Cornell University under a cooperative agreement with the National Science Foundation. The Borg was funded by a New Opportunities Grant from the Canada Foundation for Innovation. This paper makes use of data obtained from the Isaac Newton Group Archive which is maintained as part of the CASU Astronomical Data Centre at the Institute of Astronomy, Cambridge.

## REFERENCES

- Anderson, S. B., Wolszczan, A., Kulkarni, S. R., & Prince, T. A. 1997, *ApJ*, 482, 870
- Bassa, C. G., van Kerkwijk, M. H., Koester, D., & Verbunt, F. 2006, *A&A*, 456, 295
- Bégin, S., Ransom, S. M., Freire, P. C. C., Stairs, I. H., Hessels, J. W. T., Katz, J., Kaspi, V., & Camilo, F. 2008, *ApJ*, in preparation
- Bell, J. F., Bessell, M. S., Stappers, B. W., Bailes, M., & Kaspi, V. M. 1995, *ApJ*, 447, L117
- Belczynski, K., O'Shaughnessy, R., Kalogera, V., Rasio, F., Taam, R. & Bulik, T. 2008, arXiv:0712.1036v1
- Bergbusch, P. A. & Vandenberg, D. A. 1992, *ApJS*, 81, 163
- Champion, D. et al. 2008, private communication
- Damour, T. & Deruelle, N. 1985, *Ann. Inst. H. Poincaré (Physique Théorique)*, 43, 107
- Damour, T. & Deruelle, N. 1986, *Ann. Inst. H. Poincaré (Physique Théorique)*, 44, 263
- Dinescu, D., Girard, T., & van Altena, W. 1999, *ApJ*, 117, 1792
- Dowd, A., Sisk, W., & Hagen, J. 2000, in *Pulsar Astronomy - 2000 and Beyond*, IAU Colloquium 177, ed. M. Kramer, N. Wex, & R. Wielebinski, (San Francisco: Astronomical Society of the Pacific), 275
- Efron, B. & Tibshirani, R. J. 1993, *An Introduction to the Bootstrap*, (New York: Chapman & Hall)
- Faulkner, A. J. et al. 2005, *ApJ*, 618, L119
- Ferraro, F. R., Possenti, A., D'Amico, N., & Sabbi, E. 2001, *ApJ*, 561, L93
- Freire, P. C., Camilo, F., Kramer, M., Lorimer, D. R., Lyne, A. G., Manchester, R. N., & D'Amico, N. 2003, *MNRAS*, 340, 1359
- Freire, P. C., Gupta, Y., Ransom, S. M., & Ishwara-Chandra, C. H. 2004, *ApJ*, 606, L53
- Freire, P. C. C., Ransom, S. M., & Gupta, Y. 2007, *ApJ*, 662, 1177
- Freire, P. C. C., Ransom, S. M., Bégin, S., Stairs, I. H., Hessels, J. W. T., Frey, L. H., & Camilo, F. 2008, *ApJ*, 675, 670
- Harris, W. E. 1996, *AJ*, 112, 1487. See <http://www.physics.mcmaster.ca/resources/globular.html> for updated version of table.
- Hessels, J. W. T., Ransom, S. M., Stairs, I. H., Kaspi, V. M., & Freire, P. C. C. 2007, *ApJ*, 670, 363
- van den Heuvel, E. P. J. 2007, *American Institute of Physics Conference Series*, 924, 598
- Hotan, A. W., Bailes, M. & Ord, S. M. 2006, *MNRAS*, 369, 1502
- Jacoby, B. A., Hotan, A., Bailes, M., Ord, S., & Kulkarni, S. R. 2005, *ApJ*, 629, L113
- Lai, D., Bildsten, L., & Kaspi, V. M. 1995, *ApJ*, 452, 819
- Lattimer, J. M. & Prakash, M. 2007, *Phys. Rep.*, 442, 109
- Livio, M., & Pringle, J. E. 1998, *ApJ*, 505, 339
- Nice, D. J., Splaver, E. M., Stairs, I. H., Löhmer, O., Jessner, A., Kramer, M., & Cordes, J. M. 2005, *ApJ*, 634, 1242
- Nice, D. J., 2007, to appear in the proceedings of "40 Years of Pulsars: Millisecond Pulsars, Magnetars, and More", August 12-17, 2007, McGill University, Montreal, Canada, C. Bassa, Z. Wang, A. Cumming and V. Kaspi Eds.
- Odenkirchen, M., Brosche, P., Geffert, M., & Tucholke, H.-J. 1997, *New Astronomy*, 2, 477
- Press, W. H., Teukolsky, S. A., Vetterling, W. T., & Flannery, B. P. 1992, *Numerical Recipes: The Art of Scientific Computing*, 2<sup>nd</sup> edition, (Cambridge: Cambridge University Press)
- Ransom, S. M., Hessels, J. W. T., Stairs, I. H., Freire, P. C. C., Camilo, F., Kaspi, V. M., & Kaplan, D. L. 2005, *Science*, 307, 892
- Rasio, F. R. & Heggge, D. C. 1995, *ApJ*, 445, L133
- Sandquist, E. L., Bolte, M., Stetson, P. B. & Hesser, J. E. 1996, *ApJ*, 470, 910
- Scholz, R.-D., Odenkirchen, M., Hirte, S., Irwin, M. J., Borngen, F., & Ziener, R. 1996, *MNRAS*, 278, 251
- Splaver, E. M., Nice, D. J., Arzoumanian, Z., Camilo, F., Lyne, A. G., & Stairs, I. H. 2002, *ApJ*, 581, 509
- Standish, E. M. 1998, *JPL Planetary and Lunar Ephemerides, DE405/LE405*, Memo IOM 312.F-98-048, (Pasadena: JPL). <http://ssd.jpl.nasa.gov/iau-comm4/de405iom/de405iom.pdf>
- Taylor, J. H. 1992, *Philosophical Transactions of the Royal Society of London*, A, 341, 117
- Timmes, F. X., Woosley, S. E., & Weaver, T. A. 1996, *ApJ*, 457, 834
- Verbiest, J. P. W., Bailes, M., van Straten, W. Hobbs, G. B., Edwards, R. T., Manchester, R. N. Bhat, N. D. R., Sarkissian, J. M., Jacoby, B. A. and Kulkarni, S. R. 2008, *Astrophysical Journal*, in press, arXiv:0801.2589
- Webbink, R. F. 1985, in *Dynamics of Star Clusters*, IAU Symposium No. 113, ed. J. Goodman & P. Hut, (Dordrecht: Reidel), 541
- Weisberg, J. M. & Taylor, J. H. 2003, in *Radio Pulsars*, ed. M. Bailes, D. J. Nice, & S.E. Thorsett, (San Francisco: Astronomical Society of the Pacific), 93
- Wex, N. 1998, *MNRAS*, 298, 67
- Wolszczan, A., Anderson, S., Kulkarni, S., & Prince, T. 1989. IAU circular 4880
- Zacharias, N., Urban, S. E., Zacharias, M. I., Wycoff, G. L., Hall, D. M., Monet, D. G. & Rafferty, T. J. 2004, *AJ*, 127, 3043